
Prediction of dimensional accuracy and warpage of additive manufactured parts using finite element model

D. Syrlybayev¹, A. Seisekulova¹, M. Akhmetov¹, A. Perveen¹, D. Talamona¹

¹Department of Mechanical & Aerospace Engineering, School of Engineering and Digital Sciences, Nazarbayev University, Kabanbay Batyr Ave. 53, Nur-Sultan 010000 Kazakhstan

daniyar.syrlybayev@nu.edu.kz

Abstract

Fused Deposition Modelling (FDM) is one of the most affordable additive manufacturing technologies available. Although FDM printers are easy to use, the process itself is complex with nonuniform rapid heating and cooling. For this reason, complex residual stresses and part deformations are generated during the production process. Recently, the usage of simulations of the FDM process using Finite Element Analysis (FEA) to predict geometrical accuracy and residual stresses within the part has gained attention from the research community. Hence, the main objective of this study is to develop and validate a new model of the FDM process to predict dimensional deviations (length, width, and thickness), warpage, and residual stresses using FEA. To achieve the objective, thermo-mechanical analysis of a simple standard tensile test part was modelled and solved using ANSYS. To reduce the complexity of the numerical model and computational time, several important assumptions were made. The validation of the model was done against physical parts, which were manufactured using an Ultimaker S3 printer. The results have shown that with a given set of assumptions, the error between FEA predicted and experimentally measured warpage was 14.6%, while for dimensional accuracy it was found that the thickness deviation error was about 23%. Unfortunately, the current FEM model is unable to predict the length and width deviations. One of the reasons might be that the FEA model neglects the viscoelastic and viscoplastic effects. Also, the printer probably uses a compensation algorithm that is not included in the FEA model too. The possible improvements of the model, such as the inclusion of the viscoelastic and viscoplastic effects, will be discussed.

Accuracy, 3D printing, Finite Element Method (FEM), Simulation

1. Introduction

Fused deposition modelling (FDM) is the additive manufacturing process in which a filament or rod polymer is extruded through a nozzle that moves according to the programmed path. In comparison to other AM processes, it has a relatively low cost of machine and consumables and hence it is attractive for rapid prototyping.

Its process parameters determine the mechanical properties and accuracy of the manufactured part. That is why the current FDM research focused mostly on the optimization of the process parameters to achieve the best accuracy and mechanical properties.

Nowadays, numerous publications are found to focus on optimization of the strength and accuracy using Taguchi methods [1] Grey Taguchi [2] and Bayesian networks [3]. In addition, several studies were conducted to determine how each individual parameter affects a specific type of geometrical deviations. For example, [4] studied how warpage is affected by different process parameters.

As literature suggests, most of the research projects involve experimental testing, which is time consuming and provides only limited end-data. On the other hand, analytical and numerical results can help to understand how exactly deviations vary with respect to selected process parameters. Previously, few attempts were made to model the FDM process using the Finite

Element Method (FEM) [5, 6]. However, in both works each element was activated individually, which needed a fine time discretization in transient analysis and as a result significant computational effort. Hence the objective of this research is to develop a new methodology for modelling the FDM process using FEM and several simplifications described in later sections. The model was used for prediction of the dimensional deviations and warpage of standard part for tensile test. The effectiveness of the proposed method was assessed through its validation with experimental results.

The Finite Element (FE) model setup and how the experiments were conducted is also described. Then a summary of the results obtained numerically and experimentally are reported. Finally, the main trend of results is discussed, and numerical results are compared with the experimental ones. The main findings are summarized in the conclusions.

2. Methodology

To achieve the aim of the study a finite element model of the FDM process was built and validated against experimental results. The procedures for modelling and validation are described in this section.

2.1. Computational modelling

In this study, the following assumptions were used:

- The phase change, viscoelastic and viscoplastic effects were neglected
- Each layer is deposited instantly
- The manufactured part has isotropic properties with flawless microstructure
- Chamber and plate temperatures have time and space invariant values.
- Perfect bounding between the built platform and the part (no slippage)

The physical model used for simulations is shown in Figure 1. It is a dog-bone specimen for tensile test placed on the glass build platform. The specimen consists of ten layers. Each layer is 0.3 mm in thickness.

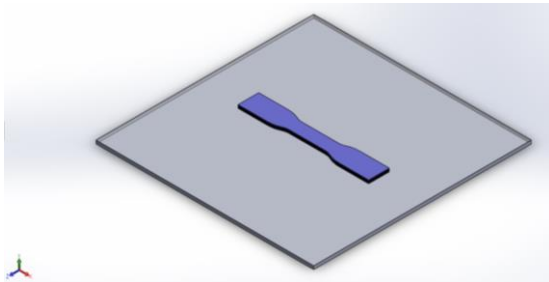


Figure 1. The model used for the simulation.

The model was meshed using ANSYS build-in automatic meshing tools. The meshing was done using 1x1x0.3 mm second-order hexahedral elements. Each element had mid-side nodes for improved accuracy. As each layer is deposited instantaneously, the model has two symmetry planes allowing to model only one quarter of the part as shown in Figure 2, which significantly reduces the computational time.

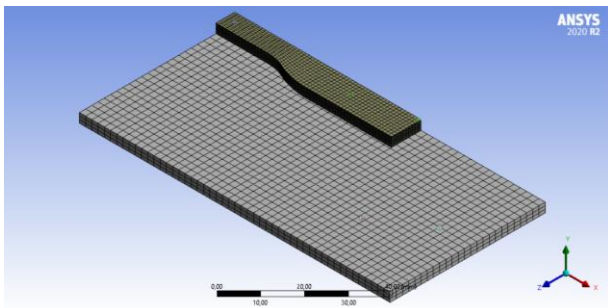


Figure 2. Model discretization.

To simulate the FDM process the thermomechanical model using the layer activation and deactivation technique was built. Its working principle is the following. When a new layer is activated the topology of the part updated and the transient thermomechanical simulation is performed on the part and the current temperature and stress distributions are used as the initial conditions [5]. This process repeats itself several times until the whole part is deposited within the simulation. Afterwards, the part is left to reach the thermal equilibrium. Finally, the constraints between the specimen and the build platform were deactivated and deformations of the part in the released conditions were obtained.

The boundary conditions for the following analysis are shown in Figure 3. The 3 mm glass platform was set at a constant temperature of 95 °C as in the real set up. The specimen and the top surface of the platform are subjected to convective heat transfer with a heat transfer coefficient of 80 W/m²K. Because

the glass platform is much stiffer than the part made of ABS it was assumed that it is rigid, and no structural analysis was conducted on it. To simulate the adhesion of the part to the glass the nodes on the lower surface of the specimen were fully constrained. This boundary condition was turned off during the detachment phase and only one node at the centre (indicated as E in Figure 3) remained constrained to prevent the rigid body motion.

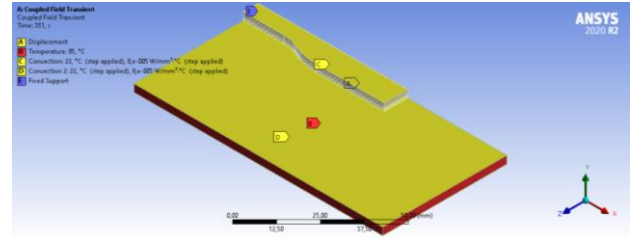


Figure 3. Boundary conditions.

As it was mentioned, the material utilized for this study is ABS. The temperature-dependent material properties were taken from [6]. In addition, a bilinear plastic model was used for this study. The validity of this model for ABS plastic was shown by [7].

2.2. Experimental Procedure

To validate the model, specimens were printed using an Ultimaker S3 (Figure 4). The key parameters used for printing are as follows: nozzle diameter was $\varnothing 0.4$ mm, temperature of extrusion was 220°C, temperature of the platform was 95°C and the ABS filament diameter was 2.85 mm. The remaining printing parameters are shown in Table 1. Three specimens were printed simultaneously to check the influence of the position. The middle position was denoted as “0” and the other two positions were denoted as “-1” and “1” respectively. Before printing, the platform was thoroughly cleaned with 80% of ethanol solution. To avoid severe warping that can lead to printing failure and nozzle damage, brims were added to the samples. After cooling and detachment, the brims were carefully cut off. The samples were measured at three different points using a digital caliper with an accuracy of 10 μ m.

Table 1 Default parameters during printing

Factor	Value	Unit
Layer thickness	0.3	mm
Wall thickness	1.3	mm
Infill density	100	%
Infill pattern	Rectilinear	-
Print speed	55	mm/s
Fan speed	2	%

The warpage was denoted as “H” and was measured from the horizontal surface at which the sample is located to the bottom side of the sample’s warped edge (Figure 5).

3. Results

In the following study, the numerical analysis was conducted and validated as described. The results of simulations and experiments are summarized in the subsections 3.1 and 3.2.

3.1. Numerical results

Using the simulation procedure described in section 2.1 the finite element analysis of the FDM was performed to find the dimensional deviations and warpage. The displacements of the part along the x, y and z axes are shown in Figures 6, 7 and 8, respectively.

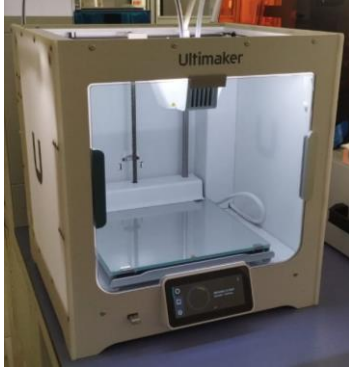


Figure 4. Ultimaker S3 printer.



Figure 5. Warped sample edge

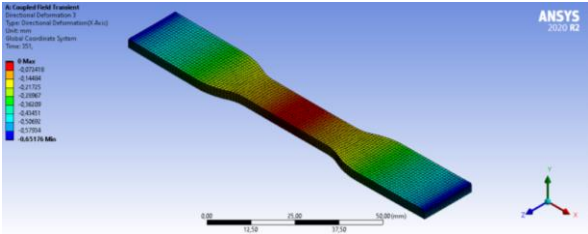


Figure 6. Deformation of the part along the x-axis

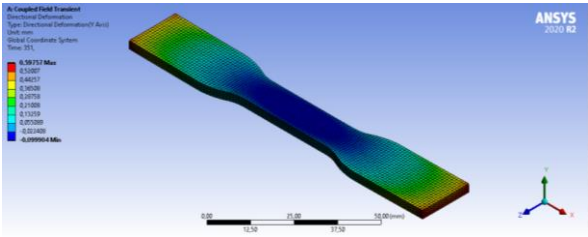


Figure 7. Deformation of the part along the y-axis

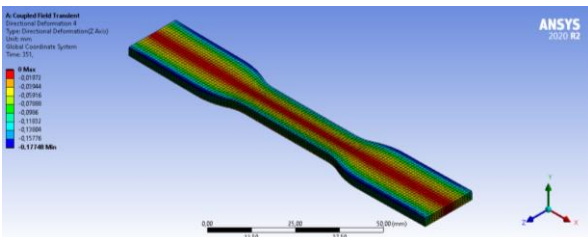


Figure 8. Deformation of the part along the z-axis

Note that the values represented in Figures 6-8 do not represent a dimensional deviation. Due to the usage of the quarter symmetry, it is necessary to multiply the values shown in Figure 6 and 8 by two to find length and width deviations (ΔL and ΔW , respectively).

The deformation along the vertical y-axis is the superposition of warpage (H) and dimensional deviation along the thickness of the part (ΔT). To find the thickness deviation following procedure was used: the corresponding deformations of the bottom and top surfaces along x-axis from $x = 0$ to $x = 60$ mm (central half-length) and along z-axis from $z = 0$ to $z = 9.5$ mm (utmost half-width) were sampled and subtracted from each

other. To find the warpage the deformation of the bottom surface was isolated. Using this procedure, the warpage and thickness deviations along the central half-length and utmost half-width were obtained and are shown in Figures 9 and 10.

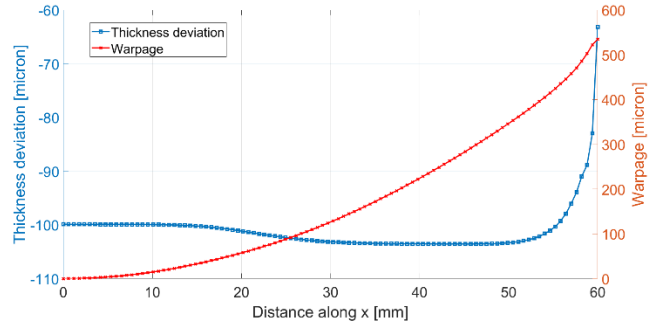


Figure 9. Warpage and thickness deviation of the part central half-length

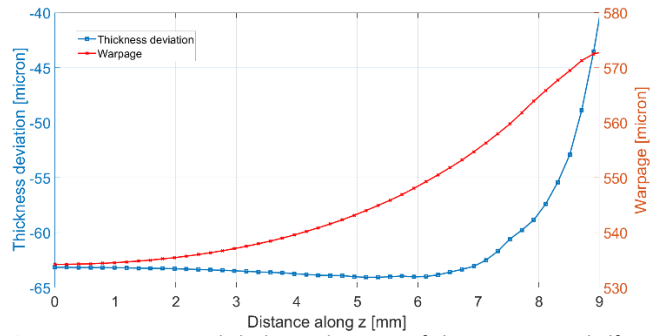


Figure 10. Warpage and thickness deviation of the part utmost half-width

From Figures 6, 7 and 8 and plots 9 and 10, the FE predicted maximum values of deviations in terms of length (ΔL), width (ΔW), thickness (ΔT), and warpage (H) have been summarized in Table 2.

Table 2 FE predicted maximum values of deviations (in μm)

ΔL	ΔW	ΔT	H
-1303	-355	-101	573

3.2. Experimental results

The influence of the position was minor. Hence, after measuring the samples and calculating the difference between the measured values and the nominal values, the resultant values were averaged and can be viewed in Table 3. The positive values of ΔL and ΔW indicate that the specimens were printed larger in length and width than the initial design. On the other hand, the negative value of thickness deviation implies that the printed samples are thinner than the digital model.

Table 3 Experimentally measured values of deviations (in μm)

ΔL	ΔW	ΔT	H
70	151	-133	501

4. Discussion

From Figures 6 and 8, both length and width deviations are negative. This happens because of the shrinkage that the part experiences while cooling.

Furthermore, Figure 7 shows that the part deforms in the vertical direction as well. The vertical deformation is associated with the shrinkage along the thickness, of each layer, and with the warpage of the part. It can be noticed that the corners of the part have the larger vertical deformation, while the centre remains relatively undeformed. Thus, the part attains the shape

of the bowl when it is detached from the built platform. This is known as warpage and its cause was described by [8]. When the material is deposited, it shrinks as it cools down. The shrinkage strain causes stress and resulting moments around the platform, which are blocked due to the constraints between the part and platform. When the part is detached, these moments cause the part to deform into a bowl shape.

Furthermore, Figures 9 and 10 show that the warpage increases with the increase in length. The shorter the dimension the smaller is the warpage. While comparing the warpage along the length and along the width, the warpage is more significant for the length direction. This phenomenon was also observed by [8]

It should be also mentioned that the thickness deviation along the length is relatively constant and is approximately $-100\ \mu\text{m}$. However, the FE model predicts that at the outer edges the thickness deviation will reduce and approach zero. This is especially true if the thickness deviation along the utmost half-width is considered. This happens because the elements located in the outer region has more faces exposed to the convective surroundings and hence FE model predicts that they will cool faster.

Considering the numerical and experimental results shown in Tables 2 and 3 it can be noticed that the planar deviations ΔL and ΔW predicted by FEM and experiment are not in agreement with each other. The experiment predicts positive deviations, while simulations results are negative ones. This might be due to the pressure from the nozzle that flattens the part and causes its dimensions to increase in size during extrusion process. In addition, it is possible that within the printer program, there might be shrinkage compensation algorithms. None of these assumptions were incorporated into the current model as it was out of the scope of this project.

The thickness deviation (ΔT) and warpage (H) predicted by the model are in good agreement with the experimental results. The errors between the values are 23% and 14.6% respectively. Experiments show larger values of the thickness deviation than the FE predictions. This might also be due to pressure acting from the extruder which flattens the molten part. Sources of errors might also include the calibration of the FDM machine and possible errors during the measurements as well as the assumptions employed during the modelling.

The Finite Element model can be improved by the inclusion of viscoelastic and viscoplastic effects and accounting for pressure acting from the nozzle to improve its planar deviation prediction.

5. Conclusion

In summary, a novel Finite Element Simulation of a ASTM part was created and the conditions of the FDM process were simulated to analyse and predict the deformation of the sample. It was found that the deviations in length and width are negative according to the FEM model and positive according to the measurements from the experimental results. The first possible explanation for such contradictions is the pressure imposed by the nozzle that leads to the flattening of the samples. Besides, the possibility of a shrinkage compensation mechanism can be another possible reason. However, the simulated and experimental results were in good agreement for thickness deviation and warpage such that the error values are 23% and 14.6% respectively.

To conclude, the model can predict thickness deformation and how much the sample can warp. The model can be improved to consider the factors that significantly affect dimensional accuracy. Thus, it will improve the ability of the model to predict planar dimensional deviations (ΔL and ΔW). This can help predict

the inaccuracies and errors reducing the wastage of material during the actual printing.

For future work, the effect of the process parameters can be considered by changing the respective values in the model to find more appropriate parameters that can mitigate the warping. The effect of nozzle pressure and shrinkage compensation mechanism can also be included in the model.

Acknowledgement:

This research was funded by Nazarbayev University under the Faculty Development Competitive Research Grant Program No 240919FD3923, "Cost effective hybrid casting methods for cellular structures".

References

- [1] Xinhua, L., Shengpeng, L., Zhou, L., Xianhua, Z., Xiaohu, C., & Zhongbin, W. (2015). An investigation on distortion of PLA thin-plate part in the FDM process. *The International Journal of Advanced Manufacturing Technology*, **79(5)** 1117-1126.
- [2] Sood, A. K., Ohdar, R. K., & Mahapatra, S. S. (2009). Improving dimensional accuracy of fused deposition modelling processed part using grey Taguchi method. *Materials & Design*, **30(10)** 4243-4252.
- [3] Mahapatra, S. S., & Sood, A. K. (2012). Bayesian regularization-based Levenberg–Marquardt neural model combined with BFOA for improving surface finish of FDM processed part. *The International Journal of Advanced Manufacturing Technology*, **60(9-12)** 1223-1235.
- [4] Panda, B. N., Shankwar, K., Garg, A., & Jian, Z. (2017). Performance evaluation of warping characteristic of fused deposition modelling process. *The International Journal of Advanced Manufacturing Technology*, **88(5-8)** 1799-1811.
- [5] Zhang, Y., & Chou, Y. K. (2006). Three-dimensional finite element analysis simulations of the fused deposition modelling process. *Proceedings of the Institution of Mechanical Engineers, Part B: Journal of Engineering Manufacture*, **220(10)** 1663-1671.
- [6] Cattenone, A., Morganti, S., Alaimo, G., & Auricchio, F. (2019). Finite element analysis of additive manufacturing based on fused deposition modeling: distortions prediction and comparison with experimental data. *Journal of Manufacturing Science and Engineering*, **141(1)**.
- [7] Rodríguez-Panes, A., Claver, J., & Camacho, A. M. (2018). The influence of manufacturing parameters on the mechanical behaviour of PLA and ABS pieces manufactured by FDM: A comparative analysis. *Materials*, **11(8)** 1333.
- [8] Armillotta, A., Bellotti, M., & Cavallaro, M. (2018). Warpage of FDM parts: Experimental tests and analytic model. *Robotics and Computer-Integrated Manufacturing*, **50** 140-152.